

KK-number non-conserving decays: Signal of $n = 2$ excitations of Extra-Dimensional Models at the LHC

Ujjal Kumar Dey^{1,2*}, Amitava Raychaudhuri^{1†}

¹⁾ *Department of Physics, University of Calcutta, 92 Acharya Prafulla Chandra Road, Kolkata 700009, India*

²⁾ *Harish-Chandra Research Institute, Chhatnag Road, Jhansi, Allahabad 211019, India*

Abstract

In the simplest universal extra-dimension models Kaluza-Klein (KK) parity distinguishes the states with odd and even KK-number. We calculate the coupling of a $2n$ -level top quark to a top quark and the Higgs scalar (both $n = 0$ states), absent at the tree level, which is mediated by strong interactions at one-loop. We show that the strength of this coupling is independent of n . We observe that the decay due to this coupling, which conserves KK-parity, can be a few per cent of the phase space suppressed decay to two n -level states which proceeds through tree-level couplings. We explore the prospects of verification of this result at the Large Hadron Collider through the production of a second-level KK top-antitop pair both of which subsequently decay to a zero mode top quark/antiquark and a Higgs boson.

PACS Nos: 11.10.Kk, 14.65.Jk, 14.80.Rt

Key Words: Universal Extra Dimension, Kaluza-Klein

I Introduction

The results of high energy experiments over the last decades, culminating in the observation of the Higgs scalar [1, 2] at the Large Hadron Collider (LHC), have continued to strengthen the confidence on the standard model (SM). Nonetheless, there are issues such as the evidence for dark matter and the confirmation of neutrino mass through several oscillation experiments which compel us to accept that there is interesting physics lying beyond the realms of the SM. One direction which has received significant attention is the possibility that there are more spacelike dimensions than the usual three – the extra-dimensional models. There is a wide variety of options here: the number of extra dimensions, whether the spacetime metric is dependent on these dimensions or not, and indeed in the possible ultraviolet completions of such theories. Here we will restrict ourselves to the simplest of these models, namely, Universal Extra Dimensions (UED).

In UED [3] besides the standard four-dimensional spacetime there are additional compact spacelike dimensions which are flat – constituting the ‘bulk’ – and all the SM particles have exposure to these. We will consider models with only one extra spacelike dimension which we denote by y . The radius

*email: ujjal.deyl@gmail.com

†email: palitprof@gmail.com

of compactification, R , sets a scale for the KK masses. The coordinate y runs from 0 to $2\pi R$. Here particles are represented by five-dimensional fields. Every such field can be Fourier expanded and expressed as a tower of four-dimensional Kaluza-Klein (KK) excitations specified by an integer n , the zero-mode being the corresponding SM particle. To reproduce the chiral nature of the zero-mode fermions a $y \leftrightarrow -y$ symmetry is imposed. Thus the extra dimension is compactified on the orbifold S^1/Z_2 . All tree-level couplings when expressed in terms of the Kaluza-Klein excitations conserve the KK-number.

Usually $1/R$ is significantly larger than the SM scale and the KK states at the n -th level have very nearly the same mass, n/R , for all particles. Thus the mass spectrum is extremely degenerate. This degeneracy is removed when the five-dimensional loop contributions [4] to the masses of the KK-states are included. To evaluate these contributions it is necessary to introduce a cut-off Λ beyond which some more fundamental theory is expected to be operational. A common practice is to choose the mass correction to be zero at this cutoff and to calculate the finite low energy contribution taking this as the boundary condition [5, 6]. A symmetry $y \rightarrow y + \pi R$ is preserved – referred to as KK-parity – and is $= (-1)^n$ for the n -th KK-level. These are the ingredients of minimal UED (or mUED).

The mUED model is completely specified by the cut-off Λ and the compactification radius R . It is known that in mUED electroweak observables receive corrections which are finite at one-loop order [7]. This justifies the comparison of the predictions of this theory with experimental data and obtaining bounds on Λ and R . Thus, from the $(g-2)$ of the muon [8], flavour changing neutral current processes [9, 10, 11], $Z \rightarrow b\bar{b}$ decay [12], the symmetry breaking ρ parameter [3, 13], and other electroweak precision tests [14, 15] it has been found that $R^{-1} \gtrsim 300\text{--}600$ GeV. A relatively modest R^{-1} encourages the continuing search for signatures of mUED at the LHC [16] and also at other future facilities [17]. Some of the more recent comparisons of UED with the data, including Dark Matter constraints, can be found in [18]. In particular, the LHC results [19] imply $R^{-1} > 600$ GeV from the multijet and missing E_T data while searches for dilepton resonances yield $R^{-1} > 715$ GeV. An analysis [19] of the CMS and ATLAS missing E_T data in the context of a model with two extra dimensions sets a limit of $R^{-1} > 600$ GeV at 99% C.L. With 10 fb^{-1} data at the 14 TeV LHC the reach of R^{-1} will be extended to 1.1 TeV for $\Lambda R = 10$ [18]. Further, Higgs boson mass and couplings when examined in the context of mUED suggest $\Lambda R \sim 6$ [20].

In this work we examine the loop-induced strong interaction mediated $t^{(2n)}t^{(0)}H^{(0)}$ vertex which respects KK-parity but does not conserve KK-number¹. Our notation is schematic here and will be sharpened later: $t^{(2n)}$ stands for any of the several top quark excitations of different chirality at the $2n$ -th level. $t^{(0)}$ and $H^{(0)}$ are the SM top quark and Higgs boson respectively. We calculate the strength of this coupling and use it in mUED to compute the decay rate of a $2n$ -level top quark to a zero mode top quark and a Higgs boson. For the top quark KK excitation this Yukawa coupling-driven decay mode will dominate over decays to other zero mode states, e.g., those with weak gauge bosons in the final state. We also compare this rate with the KK-number conserving decay to a pair of n -level states. Finally, we explore the prospects of verifying the theory at the future runs of the LHC through the detection of a signal using the pair-production of the second-level KK top quarks and their subsequent direct decays to zero mode states.

In the following section, after introducing the notations of the mUED model the calculation of the $t^{(2n)}t^{(0)}H^{(0)}$ coupling is given. This is followed by an estimation of the branching ratio of the decay of

¹KK-number non-conserving decays of the $H^{(2)}$ have been considered earlier in the context of Kaluza-Klein dark matter models [21].

the $t^{(2n)}$ state through this coupling. We then use these results to examine the possibility of detecting a second-level top-quark at the LHC through its production and decay to zero mode states. At the end, we provide a summary and some concluding remarks.

II Coupling of the $2n$ -level top quark to zero mode states

The 5-dimensional fields of UED are usually expressed in terms of a tower of 4-dimensional KK states. For example, the left- and right-chiral² quark fields of the i -th generation will be written as:

$$\mathcal{Q}_i(x, y) = \frac{\sqrt{2}}{\sqrt{2\pi R}} \left[\begin{pmatrix} u_i \\ d_i \end{pmatrix}_L(x) + \sqrt{2} \sum_{n=1}^{\infty} \left[Q_{iL}^{(n)}(x) \cos \frac{ny}{R} + Q_{iR}^{(n)}(x) \sin \frac{ny}{R} \right] \right], \quad (1)$$

$$\mathcal{U}_i(x, y) = \frac{\sqrt{2}}{\sqrt{2\pi R}} \left[u_{iR}(x) + \sqrt{2} \sum_{n=1}^{\infty} \left[U_{iR}^{(n)}(x) \cos \frac{ny}{R} + U_{iL}^{(n)}(x) \sin \frac{ny}{R} \right] \right]. \quad (2)$$

The expansion for $\mathcal{D}_i(x, y)$, containing d_{iR} , is similar to eq. (2). The fields satisfy $\mathcal{Q}_i(x, y) = -\gamma_5 \mathcal{Q}_i(x, -y)$ and $\mathcal{U}_i(x, y) = +\gamma_5 \mathcal{U}_i(x, -y)$, $\mathcal{D}_i(x, y) = +\gamma_5 \mathcal{D}_i(x, -y)$ which ensure that the zero-modes are the SM quarks with the correct chirality. For the third generation we use the notation

$$\begin{aligned} Q_{3L}^{(n)} &\equiv \begin{pmatrix} t^{(n)} \\ b^{(n)} \end{pmatrix}_L, & U_{3R}^{(n)} &\equiv t_R^{(n)}, & D_{3R}^{(n)} &\equiv b_R^{(n)}, & (n = 0, 1, \dots), \\ Q_{3R}^{(n)} &\equiv \begin{pmatrix} T^{(n)} \\ B^{(n)} \end{pmatrix}_R, & U_{3L}^{(n)} &\equiv T_L^{(n)}, & D_{3L}^{(n)} &\equiv B_L^{(n)}, & (n = 1, 2, \dots). \end{aligned} \quad (3)$$

Thus, $t_L^{(0)}, b_L^{(0)}$ are the SM third generation left-handed quarks while $t_R^{(0)}, b_R^{(0)}$ are similarly their right-handed counterparts.

In UED the mass of the n -th level KK excitation is $M_n = n/R$ irrespective of the other properties of the field so long as $1/R$ is much larger than the zero-mode mass, m_0 , which arises through the Higgs mechanism³. In mUED higher order corrections to these masses are included. In our calculation of the $t^{(2n)}t^{(0)}H^{(0)}$ coupling we use the lowest order (i.e., UED) masses of the KK states. However, when we calculate the decay rates in the next section we do include the mUED corrected masses.

As seen from eq. (3), at any KK-level n , excepting $n = 0$, there are four top-quark excitations: $t_L^{(n)}, T_R^{(n)}, T_L^{(n)}$ and $t_R^{(n)}$, the first two being members of electroweak $SU(2)$ doublets while the last two are singlets. For the zero-modes there is no right-handed doublet member, $T_R^{(0)}$, nor a left-handed singlet, $T_L^{(0)}$.

The effective coupling which we wish to calculate involves a decay of a $2n$ -level top quark to a zero mode top quark and a zero mode Higgs scalar. The $SU(2)$ doublet nature of the Higgs boson and the nonexistence of $T_R^{(0)}$ and $T_L^{(0)}$ leaves only the following possibilities $t_R^{(2n)}t_L^{(0)}H^{(0)}$ and $t_L^{(2n)}t_R^{(0)}H^{(0)}$.

The four-dimensional theory with the tower of Kaluza-Klein states is valid up to the cut-off scale Λ . The magnitude of a coupling at Λ is determined by the theory which takes over beyond this energy

²The left- and right-chiral projectors are $(1 - \gamma_5)/2$ and $(1 + \gamma_5)/2$, respectively.

³We use this approximation for all states. For the top-quark so long as $1/R \sim 1$ TeV this is not a bad approximation for our purpose.

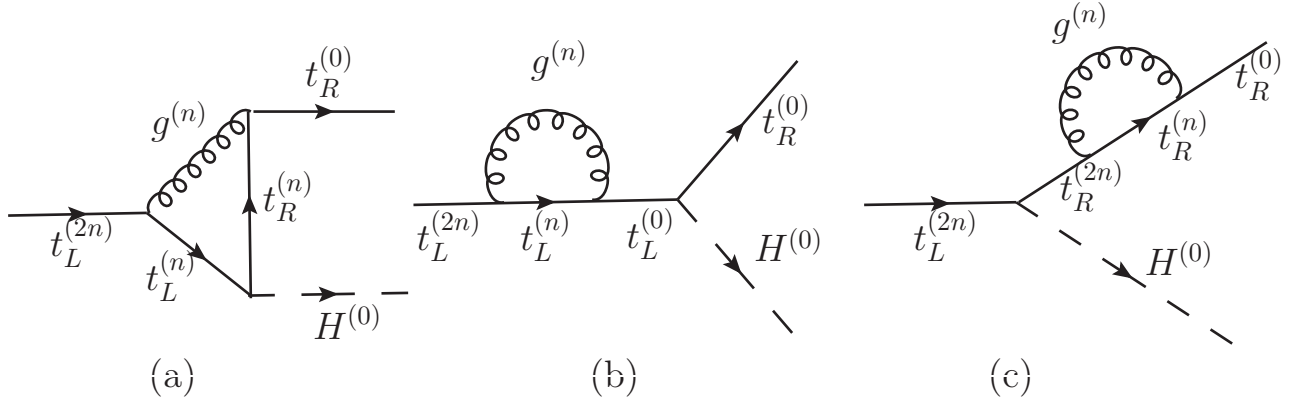


Figure 1: The dominant diagrams in the unitary gauge generating an effective $t_L^{(2n)} t_R^{(0)} H^{(0)}$ coupling.

and is to be regarded as a boundary condition for mUED. A common practice, pioneered, as noted earlier, in the context of masses of KK-states in minimal UED [5], is to take this boundary value of the coupling at Λ to be zero and obtain its magnitude at low energy through calculable corrections. We evaluate the KK-number non-conserving couplings using the same principle.

In this section we present some details of the calculation which is performed in the unitary gauge⁴. The dominant contributions to the first of these couplings⁵ will arise from the Feynman diagrams shown in Fig. 1. We ignore smaller contributions which are generated, for example, by virtual $W^{\pm(1)}$ exchange.

Each of the diagrams Fig. 1(a), 1(b), and 1(c) are individually divergent. We use dimensional regularisation to evaluate them. Using the techniques of [22] the contributions can be expressed after euclideanisation in terms of scalar loop integrals which include the divergent pieces:

$$\frac{i}{\pi^2} \int d^n q \frac{1}{[q^2 + m^2]} = m^2(-\Delta - 1 + \ln m^2) , \quad (4)$$

$$\frac{i}{\pi^2} \int d^n q \frac{1}{[q^2 + m^2][(q+p)^2 + m^2]} = \Delta + \text{finite terms} , \quad (5)$$

where

$$\Delta = -\frac{2}{n-4} + \gamma - \ln \pi , \quad \gamma = \text{Euler's constant} . \quad (6)$$

In Pauli-Villars regularisation, the momentum integral in eq. (4) is quadratically divergent while the one in eq. (5) has a logarithmic behaviour.

In presenting the contributions from the diagrams in Fig. 1 we encapsulate the couplings in a common factor:

$$\xi = - \left(\frac{g_3^2}{16\pi^2} \right) \frac{m_t}{v} (T_{ab}^c T_{ba}^c) . \quad (7)$$

⁴We have verified that identical results are obtained in the 't Hooft-Feynman gauge.

⁵The $t_R^{(2n)} t_L^{(0)} H^{(0)}$ coupling is obtained from similar diagrams – with $(L \leftrightarrow R)$ exchange – which we have not shown.

Using eqs. (4) and (5) we find for the contribution from Fig. 1(a) to be

$$\begin{aligned}
-i\mathcal{M}_1 &= \xi \bar{u}_0(k) \left\{ -\frac{1}{M_n^2} [M_n^2(-\Delta - 1 + \ln M_n^2)] \right. \\
&\quad \left. + \Delta \left(4 - \frac{1}{M_n^2} \left[2M_n^2 - \frac{3}{2}M_{2n}^2 \right] \right) + \text{finite} \right\} \frac{1-\gamma_5}{2} u_2(p) . \quad (8)
\end{aligned}$$

Above, p and k are the four momenta of the $t_L^{(2n)}$ and $t_R^{(0)}$. Similarly from Figs. 1(b) and 1(c) we respectively get

$$\begin{aligned}
-i\mathcal{M}_2 &= \xi \bar{u}_0(k) \left\{ \frac{M_{2n}^2}{M_{2n}^2 - M_0^2} \frac{1}{M_n^2} [M_n^2(-\Delta - 1 + \ln M_n^2)] \right. \\
&\quad \left. + \Delta \frac{1}{M_{2n}^2 - M_0^2} \left(-3M_{2n}^2 + \frac{1}{M_n^2} \left[\frac{1}{2}M_n^2 M_{2n}^2 - \frac{3}{2}M_{2n}^4 \right] + \text{finite} \right) \right\} \frac{1-\gamma_5}{2} u_2(p) , \quad (9)
\end{aligned}$$

and

$$\begin{aligned}
-i\mathcal{M}_3 &= \xi \bar{u}_0(k) \left\{ \frac{M_0^2}{M_0^2 - M_{2n}^2} \frac{1}{M_n^2} [M_n^2(-\Delta - 1 + \ln M_n^2)] \right. \\
&\quad \left. + \Delta \frac{1}{M_0^2 - M_{2n}^2} \left(-3M_0^2 + \frac{1}{M_n^2} \left[-\frac{1}{2}M_n^2 M_0^2 - \frac{3}{2}M_0^4 \right] + \text{finite} \right) \right\} \frac{1-\gamma_5}{2} u_2(p) . \quad (10)
\end{aligned}$$

The leading (quadratic) divergences cancel out when eqs. (8) - (10) are taken together. As remarked earlier, in the spirit of mUED calculations the boundary value of the effective $t_L^{(2n)} t_R^{(0)} H^{(0)}$ coupling is taken as zero at the scale Λ . At lower energies, μ , the net contribution is logarithmically dependent on the energy scale – i.e., proportional to $\ln(\Lambda/\mu)$ and one gets from eqs. (8) - (10):

$$\begin{aligned}
g_{t_L^{(2n)} t_R^{(0)} H^{(0)}}^{\text{eff}} &= \xi \ln \left(\frac{\Lambda}{\mu} \right) \left\{ 1 + \frac{1}{M_n^2} \left[M_n^2 \left(-2 + \frac{1}{2} \frac{M_{2n}^2 + M_0^2}{M_{2n}^2 - M_0^2} \right) + \frac{3}{2} (M_{2n}^2 - (M_{2n}^2 + M_0^2)) \right] \right\} \frac{1-\gamma_5}{2} \\
&= -\frac{1}{2} \xi \ln \left(\frac{\Lambda}{\mu} \right) \frac{1-\gamma_5}{2} , \quad (11)
\end{aligned}$$

where in the last step we have substituted $M_n = n/R$ for all n . Notice that the resultant coupling is independent of n .

III Decays of a $2n$ -level top quark

We now turn to an examination of the decay rate of a $2n$ -level KK top quark state induced through the coupling calculated in the previous section. We also compare it with other KK-number conserving decays that are allowed but are phase space suppressed.

In general for a heavy fermion F of mass m_F decaying to a different fermion f and a scalar h with masses m_f and m_h respectively the decay width is

$$\Gamma(F \rightarrow fh) = \frac{\tilde{g}^2}{8\pi m_F^3} [(m_F - m_f)^2 - m_h^2] \left\{ (m_F^2 - m_f^2 - m_h^2)^2 - 4m_h^2 m_f^2 \right\}^{1/2} . \quad (12)$$

Above, \tilde{g} is the strength of the effective Yukawa coupling between F , f , and h .

For the case at hand using eq. (11) we then have

$$\Gamma\left(t_L^{(2n)} \rightarrow t_R^{(0)} H^{(0)}\right) = \left[\frac{1}{2}\xi \ln\left(\frac{\Lambda}{\mu}\right)\right]^2 \left(\frac{2n/R}{8\pi}\right), \quad (13)$$

where we have ignored the zero-mode masses compared to $2n/R$. The mass scale μ has to be identified here with $m_F = 2n/R$.

This decay rate is to be compared with the KK-number conserving decays which proceed via tree-level couplings. As a typical example we can consider the decay $t_L^{(2n)} \rightarrow t_R^{(n)} H^{(n)}$. Here the coupling strength is simply m_t/v . This decay would have been forbidden by phase space considerations but for the mUED corrections to the KK-state masses. Keeping only the strong interaction effects for illustration⁶ the corrected mass \bar{m}_n of the n -th KK quark state is given by [5]

$$\bar{m}_n = m_n \left[1 + 3 \frac{g_3^2}{8\pi^2} \ln\left(\frac{\Lambda}{\mu}\right)\right]. \quad (14)$$

This correction has the same form for quarks of both chirality. Obviously, the Higgs scalar and its excitations receive no corrections from the strong interactions. Substituting the above in eq. (12) one has

$$\Gamma\left(t_L^{(2n)} \rightarrow t_R^{(n)} H^{(n)}\right) = \left[\frac{m_t}{v}\right]^2 \ln\left(\frac{\Lambda}{\mu}\right) \left(\frac{n/R}{16\pi}\right). \quad (15)$$

The decay width for more general possibilities such as $t_L^{(2n)} \rightarrow t_R^{(m)} H^{(2n-m)}$ can be readily obtained using the appropriate product particle masses in eq. (12).

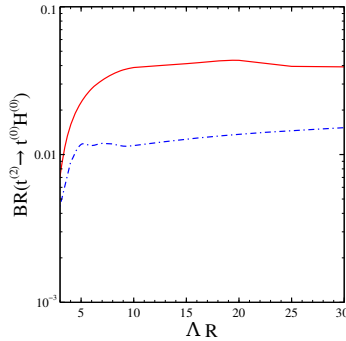


Figure 2: The branching ratio for the $t^{(2)} \rightarrow t^{(0)} H^{(0)}$ mode as a function of ΛR using the full calculation of $t^{(2)}$ decay. The red solid (blue dot-dashed) curve is for $t_L^{(2)}$ ($t_R^{(2)}$) decay.

From eqs. (7), (13), and (15) we obtain

$$\frac{\Gamma\left(t_L^{(2n)} \rightarrow t_R^{(0)} H^{(0)}\right)}{\Gamma\left(t_L^{(2n)} \rightarrow t_R^{(n)} H^{(n)}\right)} = \left[\left(\frac{g_3^2}{16\pi^2}\right) (T_{ab}^c T_{ba}^c)\right]^2 \ln\left(\frac{\Lambda}{\mu}\right) = \left[3 \left(\frac{\alpha_s}{4\pi}\right)\right]^2 \ln\left(\frac{\Lambda R}{2n}\right). \quad (16)$$

⁶For the numerical results in the following section we keep full mUED corrections [5].

The current practice is to choose Λ such that $\Lambda R \sim 10$. Masses of KK-states must not exceed Λ which implies that the above formulation is meaningful for $n \leq 5$. It bears mention that the branching ratio in eq. (16) tends to zero as $2n \rightarrow \Lambda R$.

Our interest in the next section will be to examine the possibility of detection of the KK-number non-conserving decay of second level KK top quarks after their pair production at the LHC. This decay has to compete with the KK-number conserving decays. We find that the dominant decay modes of the latter type are $t_L^{(2)} \rightarrow W^{+(1)}b_L^{(1)}, W^{+(2)}b_L^{(0)}, W^{3(1)}t_L^{(1)}, h^{0(1)}t_R^{(1)}, B^{(1)}t_L^{(1)}$ and $t_R^{(2)} \rightarrow h^{+(2)}b_R^{(0)}, h^{0(1)}t_L^{(1)}, B^{(1)}t_R^{(1)}, h^{+(1)}b_L^{(1)}$. The branching ratio for the decay $t^{(2)} \rightarrow t^{(0)}H^{(0)}$ taking into account all the KK-number conserving decay modes is shown in Fig. 2 as a function of the parameter ΛR . The red solid curve corresponds to the decay of a $t_L^{(2)}$ quark while the blue dot-dashed curve is for $t_R^{(2)}$ decay.

IV Detection prospect of the second-level KK top-quark

In this section we discuss how the $t_L^{(2)}t_R^{(0)}H^{(0)}$ coupling can be experimentally probed with particular reference to the LHC. We consider the pair production of $t_{L,R}^{(2)}\bar{t}_{R,L}^{(2)}$ at the LHC and the subsequent decay of both of them through the $t_{L,R}^{(2)}t_{R,L}^{(0)}H^{(0)}$ coupling and compare this signal with the Standard Model (SM) background⁷. Assuming that both second-level top-quarks decay in the $t^{(0)}H^{(0)}$ mode the signal consists of two top quarks⁸ and two Higgs bosons such that the correct pairing leads to identical invariant masses for the two $t^{(0)}H^{(0)}$ pairs. We estimate the Standard Model background for this channel and find it to be insignificant. However, with $\sqrt{s} = 13$ TeV and an integrated luminosity of 300 fb^{-1} the signal is small in number and inadequate for vindicating the strength of the coupling. On the other hand, with the HL-LHC option at the same \sqrt{s} with $\int \mathcal{L} dt = 3000 \text{ fb}^{-1}$ the signal could be viable. For the HE-LHC with $\sqrt{s} = 33$ TeV and $\int \mathcal{L} dt = 300 \text{ fb}^{-1}$ the reach would be more. The 100 TeV hadron FCC would obviously do the best.

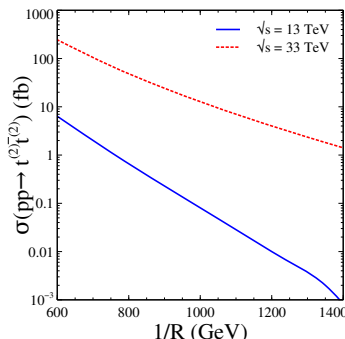


Figure 3: The production cross section for a $t^{(2)}\bar{t}^{(2)}$ pair at the LHC. The blue solid (red dashed) curve corresponds to $\sqrt{s} = 13$ TeV (33 TeV).

⁷Below we consider the signal due to the production of a $t_L^{(2)}$ along with a $\bar{t}_R^{(2)}$. Inclusion of $t_R^{(2)}\bar{t}_L^{(2)}$ production will enhance the signal by a factor of 2.

⁸Obviously, one would be a top anti-quark but we forego this distinction for ease of presentation.

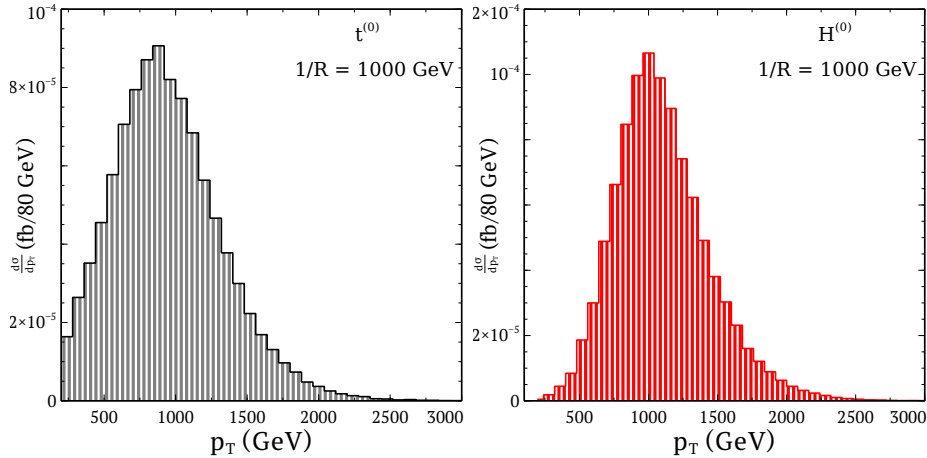


Figure 4: The p_T distributions of the top quark (left) and the Higgs boson (right) for the signal at the LHC running at $\sqrt{s} = 13$ TeV.

We use the CalcHEP implementation of mUED [23, 24] to generate the events. A parton-level Monte Carlo has been utilized with the CTEQ6l [25] distribution functions. The renormalization scale (for α_s) and the factorisation scale (for the parton distributions) are both taken⁹ as $2/R$.

The production of the $t^{(2)}\bar{t}^{(2)}$ pair proceeds through gluon-gluon fusion – both s -channel and t -channel processes – as well as $q\bar{q}$ annihilation. We find that at the \sqrt{s} that we study the former dominate. The production cross sections for LHC running at $\sqrt{s} = 13$ TeV and in the future at a 33 TeV HE-LHC are shown in Fig. 3.

The goal of this section is only to make a preliminary examination of this channel. So, we have refrained from including detailed detector simulation or indeed the subsequent decays of the top-quark or the Higgs bosons. We incorporate these effects by appropriate detection efficiency factors for these particles after applying kinematic cuts discussed later.

Since the $t^{(2)}$ states have a mass more than at least 1 TeV, the top quark and Higgs boson produced in their decays are highly boosted. Their further decay products are boosted in the direction of motion of the parent particle which results in ‘fat’ jets for the top quark and the Higgs boson which have a substructure consisting of subjets of b -quarks and light quarks and/or leptons. Since in this work we are not delving into this detailed substructure we regard the signal event as consisting of two $t^{(0)}$ and two $H^{(0)}$ fat jets. A characteristic measure of the ‘fatness’ is the opening angle parameter

$$\Delta R = \sqrt{(\Delta\eta)^2 + (\Delta\phi)^2} \quad , \quad (17)$$

where η is the pseudorapidity and ϕ the azimuthal angle. A common practice is to take $\Delta R \sim 2m/p_T$ where m is the mass of the particle [26]. As a typical example, we show in Fig. 4 the p_T distributions for the top quark and one of the Higgs bosons in the signal for $1/R = 1000$ GeV and $\sqrt{s} = 13$ TeV. It is seen that both distributions peak near 1 TeV and are small for $p_T < 500$ GeV. Therefore the four fat jets from the signal events can be expected to have ΔR around 0.35 for the top jets and 0.25 for the Higgs jets. For $1/R = 800$ GeV the p_T distribution of the fat jets is peaked at a slightly lower

⁹We have checked that if this scale is chosen as $4/R$ – to account for the production of two $t^{(2)}$ states, each of mass $2/R$ – the production cross section is enhanced by about 20%.

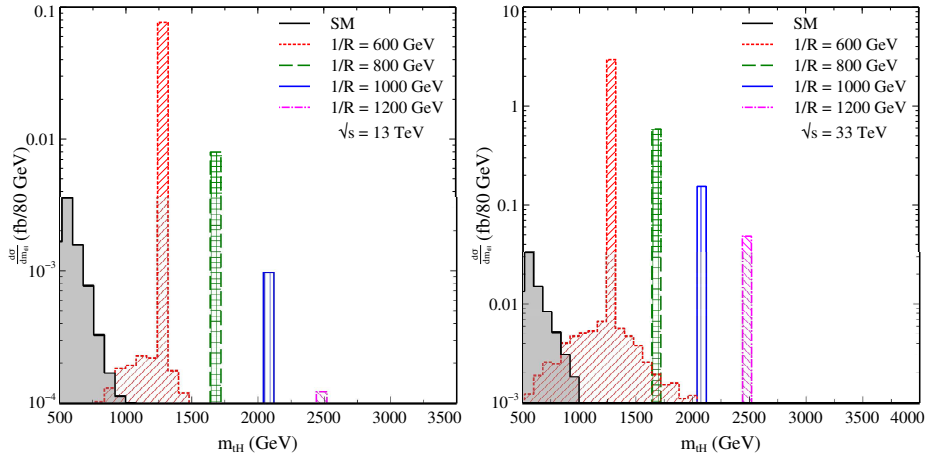


Figure 5: The cross section for the $(tH)(tH)$ signal at the LHC as a function of the $t^{(0)}H^{(0)}$ invariant mass. The histograms are for the signal at the LHC running at $\sqrt{s} = 13$ TeV (left) and 33 TeV (right) for different choices of $1/R$ (explained in the legend). The SM background is shown shaded gray in both panels.

value (~ 800 GeV). We have verified that at $\sqrt{s} = 33$ TeV these results are hardly affected. So in all cases of interest the ‘fat’ jets have $\Delta R \sim 0.30$.

For the signal as well as the background for the four jets we impose the following p_T and pseudorapidity cuts:

$$p_T > 25 \text{ GeV} \quad , \quad |\eta| < 2.5 \quad . \quad (18)$$

In addition, all four fat jets are required to be isolated. In view of our previous discussion, for any two of them i, j we require:

$$\Delta R_{ij} = \sqrt{(\Delta\eta)_{ij}^2 + (\Delta\phi)_{ij}^2} > 0.5 \quad . \quad (19)$$

From the surviving events we pick those for which there are two distinct $t^{(0)}H^{(0)}$ pairs of the same invariant mass. We ensure that the p_T of the two reconstructed $t^{(2)}$ are balanced to within 10%.

In Fig. 5 is shown the cross section for the above process as a function of the $t^{(0)}H^{(0)}$ invariant mass. In the left (right) panel are the results for $\sqrt{s} = 13$ (33) TeV. The histograms correspond to the signal for $1/R = 600$ GeV (red dotted), 800 GeV (green dashed), 1000 GeV (blue solid), and 1200 GeV (pink dot-dashed). For both panels the SM background, shown shaded gray, is insignificant in the region of the signal. So, a signal of 10 events would be strong evidence for this model.

The detection efficiency of boosted top quarks and Higgs bosons have been under much investigation in the literature. Using jet substructure features the tagging efficiency of boosted top quarks with p_T in the 800 - 1000 GeV range decaying hadronically, i.e., with a branching ratio $2/3$, is estimated around $\epsilon_{top} = 0.40-0.45$ [27]. For a boosted Higgs boson similar analyses yield an efficiency of $\epsilon_{h \rightarrow b\bar{b}} = 0.94$ for the $b\bar{b}$ decay mode [28] which has a branching ratio of about 60%.

As seen from the left panel of Fig. 5, for $\sqrt{s} = 13$ TeV with 300 fb^{-1} integrated luminosity¹⁰ the detection is unlikely. For the lowest $1/R$ that we consider, namely 600 GeV, one has around 30 events. Using the above-mentioned top quark and Higgs boson tagging efficiencies¹¹ one is left with the signal

¹⁰The expected energies and luminosities of future pp -colliders used here are from [29].

¹¹We conservatively include only the $b\bar{b}$ decay mode of the Higgs.

of $((2/3)\epsilon_{top})^2(0.6\epsilon_{h\rightarrow b\bar{b}})^2 \times 30 \sim 1$ event only. For the high luminosity HL-LHC option ($\int \mathcal{L}dt = 3000 \text{ fb}^{-1}$) this will become a healthy 10-event signal. However, with $1/R = 800 \text{ GeV}$ the signal will fall to around 1 event. On the other hand, at a HE-LHC with $\sqrt{s} = 33 \text{ TeV}$ (right panel of Fig. 5) the signal is enhanced roughly by two orders of magnitude and could remain viable till $1/R = 1 \text{ TeV}$ with $\int \mathcal{L}dt = 3000 \text{ fb}^{-1}$. We have checked that with a 100 TeV hadron FCC even for 100 fb^{-1} integrated luminosity this reach would go up to $1/R = 2.5 \text{ TeV}$ for which we find 10 events.

V Summary and Conclusions

In this work we have calculated the coupling of a $2n$ -level KK top-quark to a zero-mode top and a zero-mode Higgs boson in the universal extra-dimensional model. Such a coupling violates KK-number but respects KK-parity and is induced by loop diagrams. The dominant contribution comes from n -level quark and gluon mediation. We evaluate this coupling and show that it is independent of n .

We use this coupling to estimate the branching ratio of a second level KK-top quark for this KK-number non-conserving mode, which has the advantage of a large phase space. Considering the pair production of such second level top quarks at the LHC with $\sqrt{s} = 13 \text{ TeV}$ and 33 TeV (HE-LHC) we examine the prospects of the detection of both of them in this decay mode. Our results are encouraging for the High Luminosity or High Energy runs of the LHC. A hadron FCC with $\sqrt{s} = 100 \text{ TeV}$ would considerably expand the reach of this program.

Acknowledgements: U.K.D. is grateful to Shankha Banerjee and Tanumoy Mandal for many helpful discussions. U.K.D. is supported by funding from the Department of Atomic Energy, Government of India for the Regional Centre for Accelerator-based Particle Physics, Harish-Chandra Research Institute (HRI). A.R. is partially funded by the Department of Science and Technology Grant No. SR/S2/JCB-14/2009.

Appendix: Feynman rules

Here we list the Feynman rules relevant for our calculation. i, j are colour indices. In the first two vertices the chirality index is suppressed while in the third the colour index is not shown.

$$\begin{aligned} & \text{Diagram 1: } \text{Wavy line } g_a^{(n)} \text{ splits into } t_i^{(n)}, T_i^{(n)} \text{ and } t_j^{(2n)}, T_j^{(2n)}. \\ & \equiv -ig_s \gamma^\mu (\lambda_a)_{ij} \\ & \text{Diagram 2: } \text{Wavy line } g_a^{(n)} \text{ splits into } t_i^{(0)}, T_i^{(0)} \text{ and } t_j^{(n)}, T_j^{(n)}. \\ & \equiv -ig_s \gamma^\mu (\lambda_a)_{ij} \\ & \text{Diagram 3: } \text{Dashed line } H^{(0)} \text{ splits into } t_{R,L}^{(n)}, T_{R,L}^{(n)} \text{ and } t_{L,R}^{(n)}, T_{L,R}^{(n)}. \\ & \equiv -im_t/v \end{aligned}$$

References

- [1] G. Aad *et al.* [ATLAS Collaboration], Phys. Lett. B **718**, 1-29 (2012).
- [2] S. Chatrchyan *et al.* [CMS Collaboration], Phys. Lett. B **718**, 30-61 (2012).
- [3] T. Appelquist, H. C. Cheng and B. A. Dobrescu, Phys. Rev. D **64**, 035002 (2001) [arXiv:hep-ph/0012100]. For an alternate proposal for extra dimensions near the TeV scale, see I. Antoniadis, Phys. Lett. B **246**, 377-384 (1990).
- [4] H. Georgi, A. K. Grant and G. Hailu, Phys. Lett. B **506**, 207 (2001) [hep-ph/0012379].
- [5] H. C. Cheng, K. T. Matchev and M. Schmaltz, Phys. Rev. D **66**, 036005 (2002) [arXiv:hep-ph/0204342].
- [6] H. C. Cheng, K. T. Matchev and M. Schmaltz, Phys. Rev. D **66**, 056006 (2002) [arXiv:hep-ph/0205314].
- [7] P. Dey and G. Bhattacharyya, Phys. Rev. D **70**, 116012 (2004) [arXiv:hep-ph/0407314]; P. Dey and G. Bhattacharyya, Phys. Rev. D **69**, 076009 (2004) [arXiv:hep-ph/0309110].
- [8] P. Nath and M. Yamaguchi, Phys. Rev. D **60**, 116006 (1999) [arXiv:hep-ph/9903298].
- [9] D. Chakraverty, K. Huitu and A. Kundu, Phys. Lett. B **558**, 173 (2003) [arXiv:hep-ph/0212047].
- [10] A.J. Buras, M. Spranger and A. Weiler, Nucl. Phys. B **660**, 225 (2003) [arXiv:hep-ph/0212143]; A.J. Buras, A. Poschenrieder, M. Spranger and A. Weiler, Nucl. Phys. B **678**, 455 (2004) [arXiv:hep-ph/0306158].
- [11] K. Agashe, N.G. Deshpande and G.H. Wu, Phys. Lett. B **514**, 309 (2001) [arXiv:hep-ph/0105084].
- [12] J. F. Oliver, J. Papavassiliou and A. Santamaria, Phys. Rev. D **67**, 056002 (2003) [arXiv:hep-ph/0212391].
- [13] T. Appelquist and H. U. Yee, Phys. Rev. D **67**, 055002 (2003) [arXiv:hep-ph/0211023].
- [14] T.G. Rizzo and J.D. Wells, Phys. Rev. D **61**, 016007 (2000) [arXiv:hep-ph/9906234]; A. Strumia, Phys. Lett. B **466**, 107 (1999) [arXiv:hep-ph/9906266]; C.D. Carone, Phys. Rev. D **61**, 015008 (2000) [arXiv:hep-ph/9907362].
- [15] I. Gogoladze and C. Macesanu, Phys. Rev. D **74**, 093012 (2006) [hep-ph/0605207].
- [16] T. Rizzo, Phys. Rev. D **64**, 095010 (2001) [arXiv:hep-ph/0106336]; C. Macesanu, C.D. McMullen and S. Nandi, Phys. Rev. D **66**, 015009 (2002) [arXiv:hep-ph/0201300]; Phys. Lett. B **546**, 253 (2002) [arXiv:hep-ph/0207269]; H.-C. Cheng, Int. J. Mod. Phys. A **18**, 2779 (2003) [arXiv:hep-ph/0206035]; A. Muck, A. Pilaftsis and R. Rückl, Nucl. Phys. B **687**, 55 (2004) [arXiv:hep-ph/0312186]; B. Bhattacharjee and A. Kundu, J. Phys. G **32**, 2123 (2006) [arXiv:hep-ph/0605118]; B. Bhattacharjee and A. Kundu, Phys. Lett. B **653**, 300 (2007) [arXiv:0704.3340 [hep-ph]]; G. Bhattacharyya, A. Datta, S. K. Majee and A. Raychaudhuri, Nucl. Phys. B **821**, 48 (2009) [arXiv:hep-ph/0608208]; P. Bandyopadhyay, B. Bhattacharjee and A. Datta, JHEP **1003**, 048 (2010) [arXiv:0909.3108 [hep-ph]]; B. Bhattacharjee, A. Kundu, S. K. Rai and S. Raychaudhuri, Phys. Rev. D **81**, 035021 (2010) [arXiv:0910.4082 [hep-ph]]; B. Bhattacharjee and K. Ghosh, Phys. Rev. D **83**, 034003 (2011) [arXiv:1006.3043 [hep-ph]].

- [17] G. Bhattacharyya, P. Dey, A. Kundu and A. Raychaudhuri, Phys. Lett. B **628**, 141 (2005) [arXiv:hep-ph/0502031]; B. Bhattacharjee and A. Kundu, Phys. Lett. B **627**, 137 (2005) [arXiv:hep-ph/0508170]; A. Datta and S. K. Rai, Int. J. Mod. Phys. A **23**, 519 (2008) [arXiv:hep-ph/0509277]; B. Bhattacharjee, A. Kundu, S. K. Rai and S. Raychaudhuri, Phys. Rev. D **78**, 115005 (2008) [arXiv:0805.3619 [hep-ph]]; B. Bhattacharjee, Phys. Rev. D **79**, 016006 (2009) [arXiv:0810.4441 [hep-ph]].
- [18] G. Bertone, K. Kong, R. R. de Austri and R. Trotta, Phys. Rev. D **83**, 036008 (2011) [arXiv:1010.2023 [hep-ph]]; K. Nishiwaki, K. y. Oda, N. Okuda and R. Watanabe, Phys. Lett. B **707**, 506 (2012) [arXiv:1108.1764 [hep-ph]]; K. Nishiwaki, K. y. Oda, N. Okuda and R. Watanabe, Phys. Rev. D **85**, 035026 (2012) [arXiv:1108.1765 [hep-ph]]; G. Belanger, A. Belyaev, M. Brown, M. Kakizaki and A. Pukhov, Phys. Rev. D **87**, 016008 (2013) [arXiv:1207.0798 [hep-ph]]; S. Chang, S. Chang, S. Y. Shim and J. Song, Phys. Rev. D **86**, 117503 (2012) [arXiv:1207.6876 [hep-ph]]. T. Kakuda, K. Nishiwaki, K. y. Oda, N. Okuda and R. Watanabe, arXiv:1304.6362 [hep-ph]; T. Kakuda, K. Nishiwaki, K. y. Oda and R. Watanabe, arXiv:1305.1874 [hep-ph]; G. Servant, arXiv:1401.4176 [hep-ph].
- [19] H. Murayama, M. M. Nojiri and K. Tobioka, Phys. Rev. D **84**, 094015 (2011) [arXiv:1107.3369 [hep-ph]]; L. Edelhäuser, T. Flacke and M. Krämer, JHEP **1308**, 091 (2013) [arXiv:1302.6076 [hep-ph]]; G. Cacciapaglia, A. Deandrea, J. Ellis, J. Marrouche and L. Panizzi, Phys. Rev. D **87**, 075006 (2013) [arXiv:1302.4750 [hep-ph]].
- [20] M. Blennow, H. Melbeus, T. Ohlsson and H. Zhang, Phys. Lett. B **712**, 419 (2012) [arXiv:1112.5339 [hep-ph]]; A. Datta and S. Raychaudhuri, Phys. Rev. D **87**, 035018 (2013) [arXiv:1207.0476 [hep-ph]].
- [21] M. Kakizaki, S. Matsumoto, Y. Sato and M. Senami, Nucl. Phys. B **735**, 84 (2006) [hep-ph/0508283]; G. Belanger, M. Kakizaki and A. Pukhov, JCAP **1102**, 009 (2011) [arXiv:1012.2577 [hep-ph]], and references therein.
- [22] G. 't Hooft and M. J. G. Veltman, Nucl. Phys. B **153**, 365 (1979); G. Passarino and M. J. G. Veltman, Nucl. Phys. B **160**, 151 (1979).
- [23] A. Datta, K. Kong and K. T. Matchev, New J. Phys. **12**, 075017 (2010) [arXiv:1002.4624 [hep-ph]].
- [24] A. Belyaev, M. Brown, J. Moreno and C. Papineau, JHEP **1306**, 080 (2013) [arXiv:1212.4858].
- [25] J. Pumplin, D. R. Stump, J. Huston, H. L. Lai, P. M. Nadolsky and W. K. Tung, JHEP **0207**, 012 (2002) [hep-ph/0201195].
- [26] J. Shelton, arXiv:1302.0260 [hep-ph].
- [27] D. E. Kaplan, K. Rehermann, M. D. Schwartz and B. Tweedie, Phys. Rev. Lett. **101**, 142001 (2008) [arXiv:0806.0848 [hep-ph]].
- [28] M. Backović, T. Flacke, J. H. Kim and S. J. Lee, arXiv:1410.8131 [hep-ph].
- [29] A. Avetisyan, J. M. Campbell, T. Cohen, N. Dhirgra, J. Hirschauer, K. Howe, S. Malik and M. Narain *et al.*, arXiv:1308.1636 [hep-ex].